Quasiparticle scattering rate in a strongly polarized Fermi mixture

Rasmus Søgaard Christensen and Georg M. Bruun
Department of Physics and Astronomy, University of Aarhus, Ny Munkegade, DK-8000 Aarhus C, Denmark
(Received 4 February 2015; published 3 April 2015)

We analyze the scattering rate of an impurity atom in a Fermi sea as a function of momentum and temperature in the BCS-BEC crossover. The cross section is calculated using a microscopic multichannel theory for the Feshbach resonance scattering, including finite range and medium effects. We show that pair correlations significantly increase the cross section for strong interactions close to the unitarity regime. They give rise to a molecule pole of the cross section at negative energy on the BEC side of the resonance, which smoothly evolves into a resonance at positive scattering energy with a nonzero imaginary part on the BCS side. The resonance is the analog of superfluid pairing for the corresponding population balanced system. Using Fermi liquid theory, we show that the low temperature scattering rate of the impurity atom is significantly increased due to these pair correlations for low momenta. We demonstrate that finite range and mass imbalance effects are significant for the experimentally relevant ^{6}Li $-$ ^{40}K mixture, and we finally discuss how the scattering rate can be measured using radio-frequency spectroscopy and Bose-Fermi mixtures.

DOI: 10.1103/PhysRevA.91.042702 PACS number(s): 34.50.Cx, 67.85.Lm, 71.38.−k

I. INTRODUCTION

The scattering between quasiparticles plays a fundamental role for our understanding of many-body systems. Fermi liquid theory is based on a small quasiparticle scattering rate for low energies and temperatures [1], and quasiparticle scattering determines the transport properties of quantum systems which is of great importance for modern and future information technology. The scattering rate between electrons in two-dimensional quantum well structures has been measured [2–4], but there are few experiments providing a clean measurement of the quasiparticle scattering rate, and the inevitable presence of disorder and other complications makes a quantitative comparison with theory challenging for solid state systems [5]. A mobile impurity particle immersed in a medium with a continuous set of degrees of freedom provides a clear realization of a quasiparticle. In seminal works, Landau and Pekar demonstrated that electrons in a dielectric medium become dressed by the collective excitations of the material forming a quasiparticle called a polaron [6,7]. The study of polaron physics has subsequently grown into an independent research field [8]. Other examples of impurity quasiparticles include ^{3}He mixed with ^{4}He [1], and Λ particles in nuclear matter [9].

A major step forward in the study of impurity quasiparticles was recently made with the creation of highly population imbalanced two-component cold atomic gases. When the population of one of the components (majority atoms) is much larger than the population of the other component (minority atoms), the minority atoms play the role of the mobile impurities and the majority atoms play the role of the medium [10–12]. These experiments have lead to a renewed focus on impurity physics. A surprising result which has emerged from these studies is that the impurity atom forms a well-defined quasiparticle, coined the Fermi polaron, whose zero-momentum properties can be described accurately in terms of a rather simple theory, even for large coupling strengths [13–18]. While the polaron for zero momentum has been intensely studied both experimentally and theoretically, much less attention has been given to its properties for a nonzero momentum. In particular, the finite lifetime of a polaron with nonzero momentum due to scattering with the majority particles is almost exclusively studied in the weak coupling regime. The momentum relaxation rate of the polaron was calculated to second order in the interaction [19], and the imaginary part of the self-energy of the polaron due to collisions was calculated perturbatively to second order in the impurity-majority atom scattering length a for a broad resonance at zero temperature [20,21], as well as for temperatures much less than the Fermi temperature [22]. The momentum dependence at unitarity has also been studied [23], and the high momentum case was analyzed using the operator product expansion [24].

Here, we calculate the scattering rate of an impurity atom (polaron) with nonzero momentum on the majority fermions using a nonperturbative approach to include strong coupling effects. The Feshbach scattering between the impurity atom and the Fermi sea is described with a microscopic multichannel theory including finite range and medium effects. We analyze in detail the energy and momentum dependence of the cross section for the scattering, and show that medium effects significantly increase the cross section for strong interactions close to the unitarity regime. This is due to pair correlations giving rise to a molecule pole in the cross section at negative energy in the BEC regime ($a > 0$), which evolves smoothly into a resonance with the nonzero imaginary part at positive energy in the BCS regime ($a < 0$). This resonance is the remnant of superfluid pairing in the equivalent system with equal population of the two components. We then calculate the collision rate of the polaron with the majority atoms as a function of momentum and temperature using Fermi liquid theory. We show that it is significantly increased due to pair correlations for energies and temperatures comparable to or smaller than the Fermi energy ϵ_F of the majority particles. The effects of a nonzero effective range and a difference in the masses of the impurity and majority atoms are examined throughout, and we show that they are significant for the experimentally relevant ^{6}Li $-$ ^{40}K mixture. Finally, we discuss how the scattering rate can be measured experimentally using radio-frequency (RF) spectroscopy or Bose-Fermi mixtures.

Such a measurement would present an important step forward due to the relatively few unambiguous experimental results concerning the scattering rate of quasiparticles in the literature.

II. THEORY

Consider a single spin $\downarrow$ particle of mass $m_\downarrow$ interacting with a Fermi sea of spin $\uparrow$ particles of mass $m_\uparrow$ forming a Fermi polaron. In this paper, we investigate the collision rate between the polaron and the majority cloud using Landau Fermi liquid theory. From Fermi liquid theory, the collision rate of a single quasiparticle with momentum $\mathbf{p}_1$ with the surrounding medium is [1]

$$\frac{1}{\tau_{p_1}} = \int \frac{d^3p_2}{(2\pi)^3}\frac{m_r p_r}{8\pi^3}\int d\Omega W f_2(1-f_4), \tag{1}$$

where $W(12;34) = 2\pi^2\sigma/m_r^2$ is the transition probability for scattering of $\uparrow$ and $\downarrow$ particles with momenta $\mathbf{p}_1$ and $\mathbf{p}_2$, respectively, to momenta $\mathbf{p}_3$ and $\mathbf{p}_4$. The cross section for this process is σ, $m_r = m_\uparrow m_\downarrow/(m_\uparrow + m_\downarrow)$ is the reduced mass, and $\boldsymbol{p}_4 = \boldsymbol{p}_1 + \boldsymbol{p}_2 - \boldsymbol{p}_3$. We use units where $\hbar = k_B = 1$. Ω is the solid angle for the direction of the outgoing relative momentum $\boldsymbol{p}_r' = (m_\uparrow \boldsymbol{p}_3 - m_\downarrow \boldsymbol{p}_4)/M$ with respect to the ingoing relative momentum $\boldsymbol{p}_r = (m_\uparrow \boldsymbol{p}_1 - m_\downarrow \boldsymbol{p}_2)/M$ of the scattering process, with $M = m_\downarrow + m_\uparrow$. The distribution function is $f_p = [e^{\beta(\epsilon_{p\uparrow}-\mu)}+1]^{-1}$ with μ the chemical potential of the spin $\uparrow$ particles, and $\epsilon_{p\uparrow} = p^2/2m_\uparrow$. We can as usual for atomic gases assume that there is only s-wave scattering between $\downarrow$ and $\uparrow$ atoms, whereas there is no interaction between equal spin atoms. The focus of this paper is on medium effects on the scattering rate, and in particular the effects of pairing correlations. For this purpose it is sufficient to use $\epsilon_{p\downarrow} = p^2/2m_\downarrow$ for the polaron energy and in addition assume that it has unit quasiparticle residue. This limits our analysis to the regime $k_F|a| \lesssim 1$ where the polaron is well defined [18]. Here, $k_F = \sqrt{2m_\uparrow \epsilon_F}$ is the Fermi momentum. As we shall see, there are still strong pair correlations leading to significant effects on the cross section in this regime. Medium effects on the quasiparticle energy and residue have been investigated intensively; see, e.g., Refs. [13–16,18].

Note that whereas the polaron is the ground state on the BCS side, the ground state on the BEC side is instead a molecule formed by the $\downarrow$ atom bound to one of the $\uparrow$ atoms. We are not considering this molecular state here. Instead, we analyze the collisional properties of the so-called "repulsive" polaron, which is an excited quasiparticle state of the impurity atom on the BEC side. It is the state which is adiabatically connected to the noninteracting plane wave state in the extreme BEC limit $a \to 0_+$. The repulsive polaron is a well-defined quasiparticle with a long lifetime for $1/k_F a > 1$, and it has been examined in detail experimentally [11,12]. It is thus the collisions of the "attractive" polaron on the BCS side and the "repulsive" polaron on the BEC side that we investigate in this manuscript.

In order to describe experimentally relevant atomic systems interacting via a Feshbach resonance, we use a multichannel theory for the atom-atom scattering which includes finite range effects. Medium effects on the scattering matrix are described using the ladder approximation, which has turned out to yield surprisingly accurate results for the Fermi polaron [18]. The scattering matrix in the open channel can be written as [25]

$$\mathcal{T}(P,\omega) = \frac{\mathcal{T}_{\rm bg}}{\left(1+\frac{\Delta\mu\Delta B}{\tilde{\omega}-\Delta\mu(B-B_0)}\right)^{-1} - \mathcal{T}_{\rm bg}\Pi(P,\omega)}, \tag{2}$$

with $\boldsymbol{P} = \boldsymbol{p}_1 + \boldsymbol{p}_2$ the center-of-mass momentum, $\tilde{\omega} = \omega - P^2/2M$ is the energy in the relative frame, and $\mathcal{T}_{\rm bg} = 2\pi a_{\rm bg}/m_r$, where $a_{\rm bg}$ is the background scattering length. The width and position of the Feshbach resonance is ΔB and B_0, respectively, and the difference in magnetic moments between the Feshbach molecule and the pair of open channel scattering atoms is $\Delta\mu$. The pair propagator is

$$\Pi(P,\omega) = \int \frac{d^3q}{(2\pi)^3}\left(\frac{1-f_{k'}}{\omega + i0_+ - \frac{P^2}{2M} - \frac{q^2}{2m_r}} + \frac{2m_r}{q^2}\right), \tag{3}$$

where $\boldsymbol{k} = \frac{m_\downarrow}{M}\boldsymbol{P} + \boldsymbol{q}$ and $\boldsymbol{k}' = \frac{m_\uparrow}{M}\boldsymbol{P} - \boldsymbol{q}$. The cross section for scattering with center-of-mass momentum $\mathbf{P}$ and relative momentum $\mathbf{p}_r$ is then given by the on-shell scattering matrix as $\sigma = m_r^2|\mathcal{T}(P, P^2/2M + p_r^2/2m_r)|^2/\pi$. In a vacuum, we have $\Pi_{\rm vac}(P,\omega) = -im_r^{3/2}\sqrt{\omega - P^2/2M}/\sqrt{2}\pi$, and the on-shell $\mathcal{T}$ matrix Eq. (2) becomes

$$\mathcal{T}_{\rm vac} = \frac{2\pi a/m_r}{\frac{p_r^2 r_{\rm eff}(a-a_{\rm bg})/2-1}{p_r^2 r_{\rm eff} a_{\rm bg}(1-a_{\rm bg}/a)/2-1} + ip_r a}. \tag{4}$$

The effective range is $r_{\rm eff} = -(m_r a_{\rm bg}\Delta\mu\Delta B)^{-1}$ and we have used the usual relation $a = a_{\rm bg}[1 - \Delta B/(B - B_0)]$. In the limit $p_r r_{\rm eff} \ll 1$, Eq. (4) reduces to $\mathcal{T} = 2\pi a/m_r(1 + ip_r a)$ for a broad Feshbach resonance.

III. CROSS SECTION

In Fig. 1, we plot the cross section σ in units of $4\pi k_F^{-2}$ for a broad resonance with $k_F r_{\rm eff} = 0$ as a function of scattering energy ω and scattering length a. We have chosen the case of equal masses $m_\uparrow = m_\downarrow$. The center-of-mass momentum is

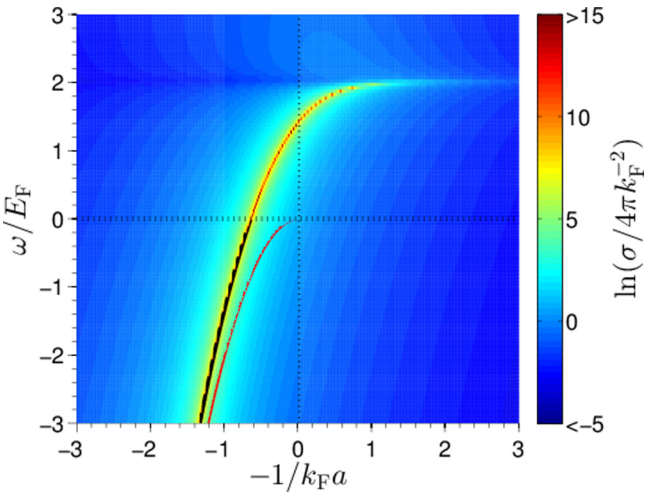

FIG. 1. (Color online) The $\mathbf{P} = 0$ cross section σ in units of $4\pi k_F^{-2}$ as a function of the energy ω and scattering length a for $T = 0.01\,T_F$, $m_\downarrow = m_\uparrow$, and $k_F r_{\rm eff} = 0$. The black line is the numerically obtained pole of the scattering matrix, while the red line is the molecule pole in a vacuum given by $\epsilon_B = -1/2m_r a^2$.

zero, $P = 0$, and the temperature is very low with $T = 0.01\epsilon_F$. Zero energy corresponds to the bottom of the Fermi sea of the spin $\uparrow$ atoms. We see a clear pole in the cross section for negative energy on the BEC side of the resonance. It comes from the molecule pole which is pushed to higher energies by medium effects, compared to the vacuum molecule energy $\epsilon_B = -1/2m_r a^2$. The ladder approximation employed here provides a qualitatively correct description of the medium energy shift which is sufficient for the present purpose, although there are quantitative corrections [15,16,18]. The molecule pole is undamped for negative energy whereas it acquires an imaginary part becoming a resonance for $\omega > 0$ and $T > 0$. This is because the molecule can dissociate into atom pairs with opposite momenta for positive energy. For $T = 0$, the molecule is stable up to the energy $2\epsilon_F$ with the pole having no imaginary part, since Fermi blocking prohibits dissociation for $\omega \leqslant 2\epsilon_F$. Indeed, a straightforward calculation yields

$$\mathrm{Im}[\Pi(P = 0,\omega)] = -\frac{m_r}{2\pi}\sqrt{2m_r\omega}[1 - f(2m_r\omega)], \qquad (5)$$

for the imaginary part of the pair propagator describing the decay of the molecule.

Note that the scattering processes in Eq. (1) of course all occur at positive energy. In Fig. 1 we nevertheless plot the cross section at negative energies as well to illustrate how the molecule pole at negative energy on the BEC side smoothly develops into a resonance of the cross section at positive energy on the BCS side. In the weak coupling BCS limit $k_F a \to 0_-$, the resonance position is located at twice the Fermi energy, $\omega = 2\epsilon_F$. The resonance is due to pair correlations, and it is the polaron analog of the Cooper pole for a balanced system with $n_\uparrow = n_\downarrow$. Contrary to the case of a population balanced system where there is a real undamped pole at twice the Fermi energy at the critical temperature for superfluidity, there is no true pole in the BCS regime of the polaron due to the strong population imbalance. Importantly, we see from Fig. 1 that the cross section is significantly increased for energy and momentum in the vicinity of the Cooper resonance. This effect is most pronounced close to the unitarity regime whereas it is small in the BEC and BCS limits. The increase in the cross section is important for low temperatures $T \ll \epsilon_F$, whereas our numerical calculations (not shown here) demonstrate that the Cooper resonance becomes more and more broad with increasing T. As expected, it eventually vanishes in the classical limit $T \gg \epsilon_F$ where the cross section is given by its vacuum value $\sigma_{vac} = m_r^2|\mathcal{T}_{vac}|^2/\pi$.

The Fermi polaron has recently been investigated experimentally with ^{40}K impurity atoms in a Fermi sea of ^{6}Li atoms. The atoms were interacting via a Feshbach resonance with an effective range $k_F r_{eff} \simeq -1.8$ [11]. In Fig. 2, we therefore plot the cross section for the parameters of this system: $m_\downarrow/m_\uparrow = 40/6$, $k_F r_{eff} = -1.8$, and a very low temperature of $T = 0.01\,\epsilon_F$. We see that the qualitative behavior is the same as for a broad resonance with mass balance: There is a real molecule pole at negative energy on the BEC side which smoothly develops into a Cooper resonance with a nonzero imaginary part at positive energy on the BCS side. In the BCS limit $k_F a \to 0_-$, the resonance is located at

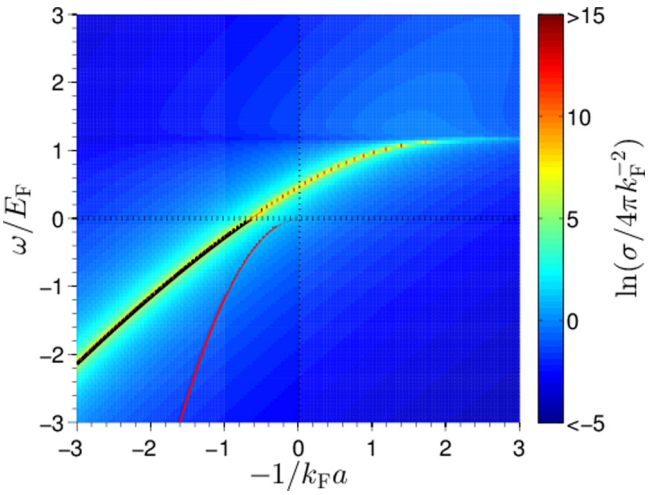

FIG. 2. (Color online) The cross section σ in units of $4\pi k_F^{-2}$ as a function of total energy ω and scattering length a for $T = 0.01\,\epsilon_F$, $m_\downarrow/m_\uparrow = 40/6$, and $k_F r_{eff} = -1.8$ relevant for the recent experiment using a ^{40}K − ^{6}Li mixture [11]. The black line is the numerically obtained pole of the scattering matrix, while the red line is the molecule pole in a vacuum given by $\epsilon_B = -1/2m_r a^2$.

$\omega = (1 + m_\downarrow/m_\uparrow)\epsilon_F$ corresponding to pairing between states at opposite sides of the Fermi surface. Comparing Figs. 1 and 2 demonstrates that mass imbalance and a nonzero finite range moves the region of an increased cross section due to medium effects towards the BCS side as compared to the case of a broad resonance with mass balance. In other words, the position of the molecule pole and Cooper resonance is moved towards the BCS side. This asymmetry due to a finite range and mass imbalance effects is consistent with what is found for other properties of the polaron [18].

We plot in Fig. 3 the cross section σ in units of the vacuum cross section σ_{vac} as a function of the scattering center-of-mass and relative momenta for a broad resonance with $m_\uparrow = m_\downarrow$ and $k_F a = \pm 1$. The temperature is $T = 0.01\,T_F$. The cross section is significantly increased compared to its vacuum value for momenta corresponding to energies close to the Cooper resonance. For $k_F a = 1$, this gives rise to a large region of enhanced scattering for momenta $\lesssim k_F$, since the molecule pole and Cooper resonance are moved to positive energies by medium effects on the BEC side, as seen in Fig. 1. On the BCS side with $k_F a = -1$, we see that the Cooper resonance gives rise to a sharp increase in the scattering rate for $P \simeq 0$ and $p_r \simeq k_F$. In the weak coupling BCS limit $k_F a \to 0_-$, the Cooper resonance is located at $P = 0$ and $p_r = k_F$, which demonstrates that even in this extreme imbalanced case, the largest pairing correlations are for momenta at opposite sides of the Fermi surface of the majority particle. We furthermore see that the Cooper resonance vanishes with increasing center-of-mass momentum. There is therefore no trace of a possible Fulde-Ferrel-Larkin-Ovchinikov effect on the cross section for this imbalanced system. Our numerical calculations show that the resonance in the cross section becomes sharper with decreasing temperature, but that it never becomes a real pole since there is no Cooper instability in this strongly imbalanced limit.

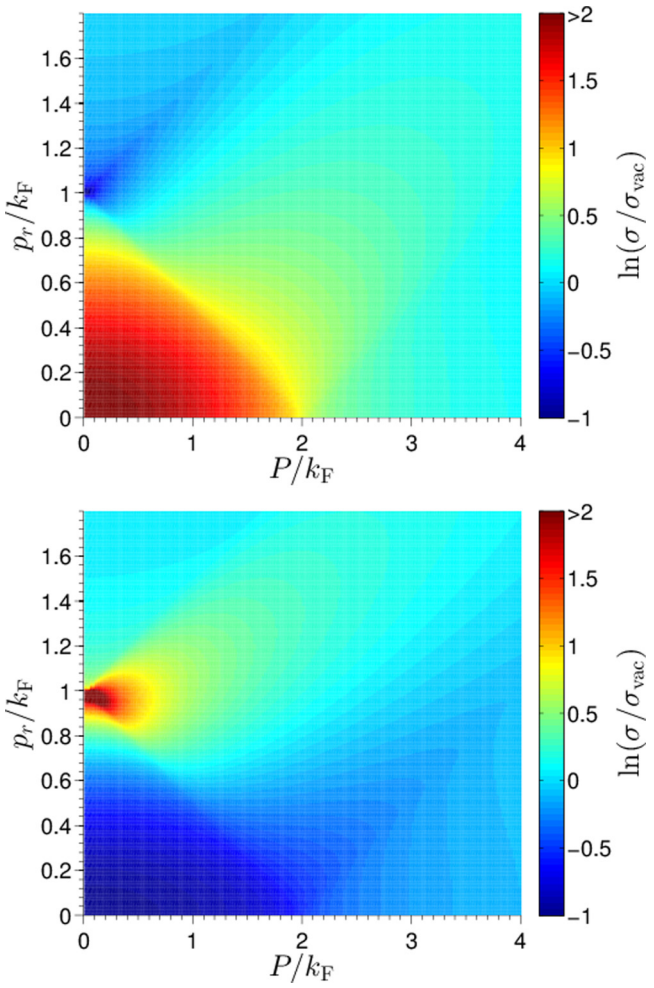

FIG. 3. (Color online) The cross section for $k_F a = +1$ (top) and $k_F a = -1$ (bottom) relative to vacuum cross section for $T = 0.01\ T_F$, $m_\downarrow = m_\uparrow$, and $k_F r_{eff} = 0$.

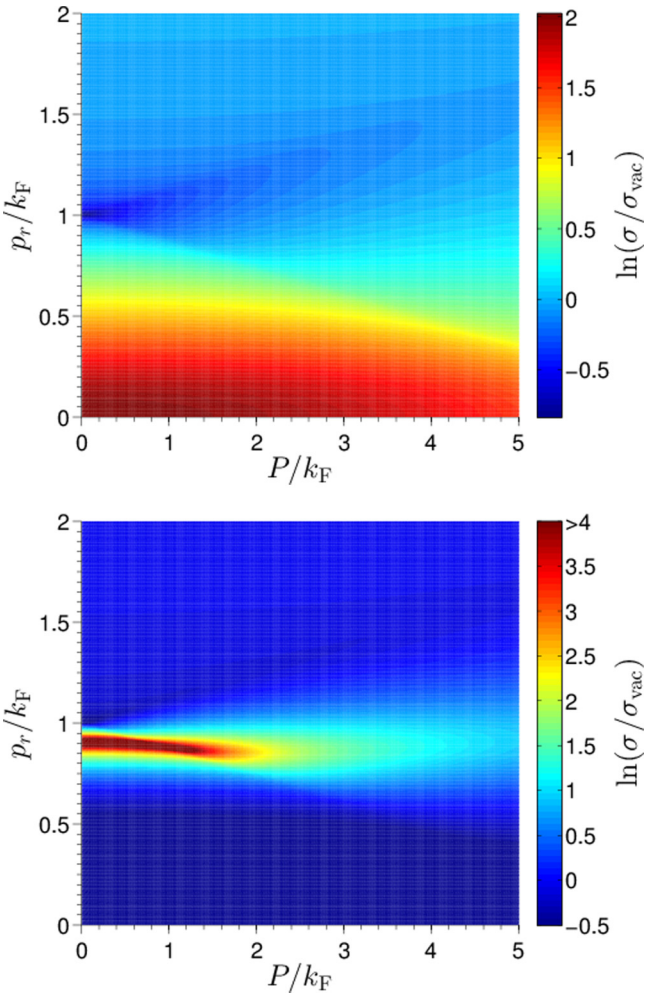

FIG. 4. (Color online) The cross section for $k_F a = +1$ (top) and $k_F a = -1$ (bottom) relative to vacuum cross section for $T = 0.01\ T_F$, $m_\downarrow/m_\uparrow = 6.6$, and $k_F r_{eff} = -1.8$.

In Fig. 4, we plot the cross section as a function of the scattering momenta for the experimentally relevant case of a ^{40}K impurity atom in a Fermi sea of ^{6}Li atoms taking $k_F a = \pm 1$ and $T = 0.01\,\epsilon_F$. The physics is again qualitatively the same as for the case of a broad resonance with mass balance. In particular, we see that the Cooper resonance on the BCS side is located at $P \simeq 0$ and $p_r \simeq k_F$. This shows that the strongest pair correlations are still located on opposite sides of the majority Fermi sea, even for a large mass imbalance as we already noted above. The cross section is increased much more on the BCS side for the case of a finite range and mass imbalance compared to a broad resonance with mass balance, as can be seen by comparing the scales in Figs. 3 and 4 (bottom). This is again consistent with the general observation that a finite range and mass imbalance moves medium effects toward the BCS side.

IV. COLLISION RATE

We now analyze how the increase in the cross section due to pair correlations manifests itself in the collision rate of the polaron. This rate is obtained from the appropriate momentum average of the cross section given in Eq. (1), and we will calculate it as a function of momentum and temperature.

In Fig. 5, we plot the collision rate in units of ϵ_F as a function of momentum for $k_F a = \pm 1$ for a very low temperature $T = 0.01\ \epsilon_F$. We show both the case of a broad resonance with mass balance, and the experimentally relevant case corresponding to a ^{40}K impurity atom colliding with a Fermi sea of ^{6}Li atoms. Consider first the case of a broad resonance with mass balance. Comparing with the "vacuum" collision rate defined as the rate obtained using the vacuum cross section in Eq. (1), we see that medium effects indeed increase the scattering rate due to pair correlations. The effect is largest on the BEC side. Note that the vacuum cross section is the same for $k_F a = \pm 1$ for a broad resonance. Consider next the narrow resonance for which there is no symmetry between the vacuum cross section at $k_F a = \pm 1$. Figure 5 shows that the significant increase in the collision rate due to pairing correlations is now largest on the BCS side with $k_F a = -1$. This difference in the medium effects on the collision rate between the broad and the narrow resonance is consistent with what we found for the cross section. In particular, we see that the increase in the scattering rate due to medium effects is much more pronounced for the narrow

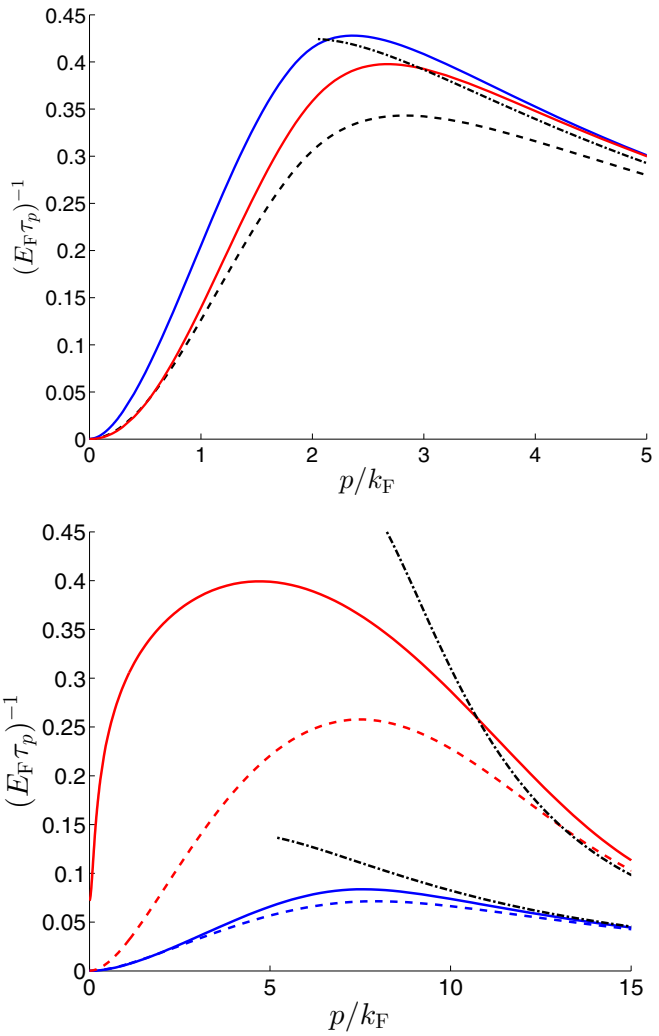

FIG. 5. (Color online) The collision rate of the polaron as a function of momentum for $T = 0.01\ \epsilon_F$ and for $k_F r_{eff} = 0$ with equal masses $m_\downarrow = m_\uparrow$ (top), and the case relevant to the ^{6}Li − ^{40}K mixture with $k_F r_{eff} = -1.8$ and $m_\downarrow/m_\uparrow = 6.6$ (bottom). In both figures, the solid blue line is for $k_F a = +1$, the solid red line is for $k_F a = -1$, dashed lines are the vacuum rate, and the dash-dotted lines are the $p \gg k_F$ limit given by Eq. (6).

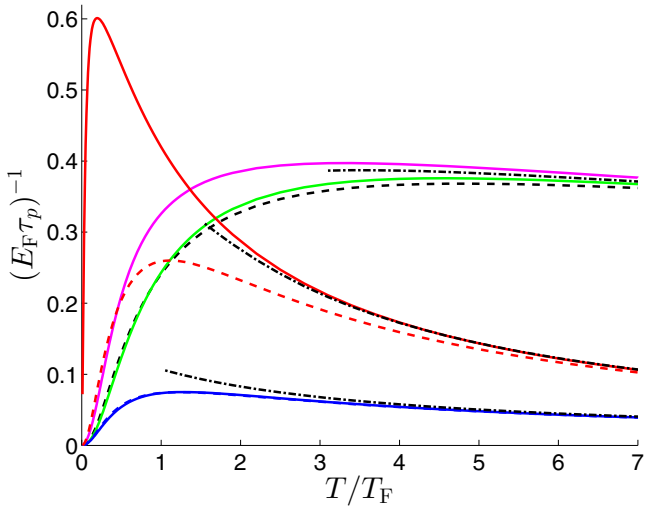

FIG. 6. (Color online) The collision rate of the polaron as a function of temperature for $p = 0$. The dashed lines are the vacuum rate; the dash-dotted lines are the $p \gg k_F$ limit. The remaining lines are for $k_F r_{eff} = 0$ with equal masses $m_\downarrow = m_\uparrow$ and $k_F a = +1$ (magenta) and $k_F a = -1$ (green), and the case relevant to the ^{6}Li − ^{40}K mixture with $k_F r_{eff} = -1.8$, $m_\downarrow/m_\uparrow = 6.6$ and $k_F a = +1$ (blue) and $k_F a = -1$ (red).

resonance on the BCS side. The reason is that the Cooper resonance has moved towards the BCS side as we saw in Figs. 2 and 4. Since the resonance is located at momenta around the Fermi sea, which are precisely those important for the collision rate, this leads to the large effects shown in Fig. 5.

We also see that the medium effects are most significant for low momenta. Intriguingly, the numerical calculations indicate that the momentum dependence of the collision rate at small p is changed by medium effects. This opens up the interesting but challenging problem of examining the low p dependence of the collision rate analytically in order to extract the power law. For high momenta on the other hand, the scattering rate approaches its classical value. This is as expected, since Fermi blocking becomes insignificant for large momenta. The collision integral (1) can in fact be solved analytically in the limit $p \gg k_F, \sqrt{2m_\uparrow T}$ yielding

$$\frac{1}{\tau_p} = \frac{4\pi n_\uparrow}{m_\downarrow} \frac{a^2 p}{\left(\frac{(\frac{m_\uparrow}{M})^2 p^2 r_{eff}(a-a_{bg})-2}{(\frac{m_\uparrow}{M})^2 p^2 r_{eff} a_{bg}(1-a_{bg}/a)-2}\right)^2 + \left(\frac{m_\uparrow}{M} ap\right)^2}$$
$$= \frac{4\pi n_\uparrow}{m_\downarrow} \frac{a^2 p}{1 + \left(\frac{m_\uparrow}{M} ap\right)^2}, \tag{6}$$

where the last line holds for a broad resonance. From Fig. 5, we see that the collision rates approach this expression for high momenta confirming the accuracy of our numerics.

We note that pair correlations have been shown to lead to a similar increase in the collision rate for a population balanced system, which strongly affects the damping of collective modes [26–28], the shear viscosity, and the spin diffusion constant [29–31].

The temperature dependence of the collision rate is plotted in Fig. 6 for zero momentum in units of ϵ_F. We have as before taken $k_F a = \pm 1$ and analyzed a broad resonance with mass balance as well as the experimentally relevant case of a ^{40}K atom in a ^{6}Li Fermi sea. Again, we see by comparing with the value obtained using the vacuum cross section σ_{vac} that pairing correlations significantly increase the collision rate for low temperatures. Consistent with the results above, medium effects are most significant on the BEC side for the wide resonance whereas they are most significant on the BCS side for the narrow resonance. In addition, as we saw for the momentum dependence, medium effects are largest for a narrow resonance on the BCS side. The reason for this is the same as for the momentum dependence discussed above: The Cooper resonance has moved towards the BCS side for the narrow resonance and is located at momenta close to the Fermi sea, which are the most important for the collision rate.

Figure 6 furthermore indicates that the low T dependence of the collision rate is changed due to medium effects. As for the low p dependence, it would be an interesting but challenging problem to examine this analytically in order to extract the power law describing the low T dependence. For high temperatures $T \gg \epsilon_F$, the effects of pairing correlations vanish and the scattering rate approaches its classical value. The integral in (1) can be solved in the classical limit, and we obtain

$$\frac{1}{\tau_p} = 2n_\uparrow \sqrt{\frac{2T}{\pi m_\uparrow}} \bar{\sigma}, \tag{7}$$

for $p \ll \sqrt{m_\downarrow^2 T/m_\uparrow}$. Here

$$\begin{aligned} \bar{\sigma} &= 8\pi a^2 \int_0^\infty dx \frac{x^3 e^{-x^2}}{\left(\frac{T r_{\rm eff}(a-a_{\rm bg})x^2 - 2T_a a^2}{T r_{\rm eff} a_{\rm bg}(1-a_{\rm bg}/a)x^2 - 2T_a a^2}\right)^2 + \frac{T}{T_a}x^2} \\ &= 8\pi a^2 \int_0^\infty dx \frac{x^3 e^{-x^2}}{1+\frac{T}{T_a}x^2} \end{aligned} \tag{8}$$

is an effective cross section, and T_a is defined as

$$T_a = M^2/2m_\uparrow m_\downarrow^2 a^2. \tag{9}$$

The last line in Eq. (8) holds for a broad resonance. For a broad resonance, Eq. (8) yields $\bar{\sigma} = 4\pi a^2$ for the effective cross section in the weak coupling limit $T_a \gg T$, and $\bar{\sigma} = 2\pi M^2/m_\uparrow m_\downarrow^2 T$ in the strong coupling limit $T_a \ll T$. This gives

$$\frac{1}{\tau_{p\downarrow}} = 4n_\uparrow \sqrt{\frac{2\pi}{m_\uparrow}} \times \begin{cases} 2a^2\sqrt{T} & \text{for} \quad T_a \gg T \\ \frac{m_\uparrow}{m_r^2}\frac{1}{\sqrt{T}} & \text{for} \quad T_a \ll T. \end{cases} \tag{10}$$

Figure 6 shows as expected that the collision rates approach the classical value for $T \gg \epsilon_F$ given by Eq. (10), confirming the accuracy of our numerics.

V. EXPERIMENTAL OBSERVATION

We now briefly discuss how the collision rate of the impurity atom can be detected experimentally. One method is to use RF spectroscopy to Rabi flip the impurity atom between an internal state interacting with the majority Fermi sea and a noninteracting internal state. The collisions of the impurity atom when it is in the interacting state cause decoherence which results in a damping of the Rabi oscillations. This damping has in fact already been observed experimentally in the $^{40}K - {}^6Li$ mixture [11]. Using this, one can extract the collision rate from the measured decoherence rate. The collision rate can also be measured using Bose-Fermi mixtures. One could create a Bose-Einstein condensate of impurity atoms in a finite momentum state which then collides with the majority Fermi sea. The advantage of this method is that the polaron is then in a definite momentum state. However, there will be nontrivial effects on the scattering rate due to the presence of the BEC which must be examined.

VI. CONCLUSIONS

We have analyzed the scattering rate of an impurity atom with nonzero momentum in a Fermi sea of majority atoms. The cross section for the Feshbach resonance mediated interaction was calculated using a microscopic multichannel theory, which includes finite range and medium effects. We demonstrated that correlations between states with opposite momenta significantly increase the cross section. These correlations are due to molecule formation at negative energy on the BEC side of the resonance, which smoothly connects to a Cooper pair resonance on the BCS side for energies and momenta comparable to the Fermi energy. They are the polaron analog of superfluid pairing for the corresponding population balanced system. We demonstrated that the pair correlations lead to a considerable increase in the low temperature scattering rate, for impurity momenta smaller than or comparable to the Fermi momentum of the majority atoms. The effects of mass imbalance and a finite range of the interaction were shown to be significant for the experimentally relevant $^6Li - {}^{40}K$ mixture. Finally, we discussed how the scattering rate of an impurity atom can be measured using RF spectroscopy or Bose-Fermi mixtures.

ACKNOWLEDGMENTS

We acknowledge useful discussions with Marko Cetina. We would like to acknowledge the support of the Hartmann Foundation via Grant No. A21352 and the Villum Foundation via Grant No. VKR023163.

[1] G. Baym and C. Pethick, *Landau Fermi-Liquid Theory: Concepts and Applications* (Wiley-VCH, Weinheim, 1991).
[2] Y. Berk, A. Kamenev, A. Palevski, L. N. Pfeiffer, and K. W. West, Phys. Rev. B **51**, 2604 (1995).
[3] S. Q. Murphy, J. P. Eisenstein, L. N. Pfeiffer, and K. W. West, Phys. Rev. B **52**, 14825 (1995).
[4] M. Slutzky, O. Entin-Wohlman, Y. Berk, A. Palevski, and H. Shtrikman, Phys. Rev. B **53**, 4065 (1996).
[5] Z. Qian and G. Vignale, Phys. Rev. B **71**, 075112 (2005).
[6] L. D. Landau, Phys. Z. Sowjetunion **3**, 644 (1933).
[7] S. I. Pekar, Zh. Eksp. Teor. Fiz. **16**, 335 (1946).
[8] G. Mahan, *Many-Particle Physics* (Kluwer Academic/Plenum Publishers, New York, 2000).
[9] R. Bishop, Annals of Physics **78**, 391 (1973).
[10] A. Schirotzek, C.-H. Wu, A. Sommer, and M. W. Zwierlein, Phys. Rev. Lett. **102**, 230402 (2009).
[11] C. Kohstall, M. Zaccanti, M. Jag, A. Trenkwalder, P. Massignan, G. M. Bruun, F. Schreck, and R. Grimm, Natural (London) **485**, 615 (2012).
[12] M. Koschorreck, D. Pertot, E. Vogt, B. Fröhlich, M. Feld, and M. Köhl, Nature (London) **485**, 619 (2012).
[13] F. Chevy, Phys. Rev. A **74**, 063628 (2006).

[14] C. Lobo, A. Recati, S. Giorgini, and S. Stringari, Phys. Rev. Lett. **97**, 200403 (2006).
[15] M. Punk, P. T. Dumitrescu, and W. Zwerger, Phys. Rev. A **80**, 053605 (2009).
[16] N. Prokof'ev and B. Svistunov, Phys. Rev. B **77**, 020408 (2008).
[17] C. J. M. Mathy, M. M. Parish, and D. A. Huse, Phys. Rev. Lett. **106**, 166404 (2011).
[18] P. Massignan, M. Zaccanti, and G. M. Bruun, Rep. Prog. Phys. **77**, 034401 (2014).
[19] G. M. Bruun, A. Recati, C. J. Pethick, H. Smith, and S. Stringari, Phys. Rev. Lett. **100**, 240406 (2008).
[20] C. Trefzger and Y. Castin, EPL (Europhysics Letters) **104**, 50005 (2013).
[21] C. Trefzger and Y. Castin, Phys. Rev. A **90**, 033619 (2014).
[22] Z. Lan, G. M. Bruun, and C. Lobo, Phys. Rev. Lett. **111**, 145301 (2013).
[23] J. J. Kinnunen, Phys. Rev. A **85**, 012701 (2012).
[24] Y. Nishida, Phys. Rev. A **85**, 053643 (2012).
[25] G. M. Bruun, A. D. Jackson, and E. E. Kolomeitsev, Phys. Rev. A **71**, 052713 (2005).
[26] S. Riedl, E. R. Sánchez Guajardo, C. Kohstall, A. Altmeyer, M. J. Wright, J. H. Denschlag, R. Grimm, G. M. Bruun, and H. Smith, Phys. Rev. A **78**, 053609 (2008).
[27] S. K. Baur, E. Vogt, M. Köhl, and G. M. Bruun, Phys. Rev. A **87**, 043612 (2013).
[28] M. Urban, S. Chiacchiera, D. Davesne, T. Enss, and P.-A. Pantel, J. Phys.: Conference Series **497**, 012028 (2014).
[29] G. M. Bruun and H. Smith, Phys. Rev. A **72**, 043605 (2005).
[30] T. Enss, C. Küppersbusch, and L. Fritz, Phys. Rev. A **86**, 013617 (2012).
[31] T. Enss, Phys. Rev. A **88**, 033630 (2013).